Eur Biophys J (2001) 29: 587–596
DOI 10.1007/s002490000116

ARTICLE

Arthur Vermeulen · Jean-Pierre Rospars

Membrane potential and its electrode-recorded counterpart in an electrical model of an olfactory sensillum

Received: 8 March 2000 / Revised version: 25 September 2000 / Accepted: 25 September 2000 / Published online: 20 December 2000

Abstract Insect receptor neurons are surrounded with auxiliary cells and encased in a hair. Their electrical activity is usually recorded with an electrode located at the tip of the hair. Analytical expressions giving the membrane potential along the sensory dendrite and the tip-recorded potential are derived for a neuron in steady-state conditions. They formally close the gap between theoretical models and experimental measurements, when transduction mechanisms and active membrane properties are not taken into account. It is shown that the tip-recorded potential reflects correctly the relative variations of the dendritic membrane potential as a function of stimulus intensity over a large range of parameters. The geometric and electrical characteristics of the sensillum that need be known to compute the dendritic membrane potential from the tip-recorded potential are given.

Key words Olfactory sensory neuron · Intensity coding · Receptor potential · Cable equation · Single neuron modeling

Introduction

Odorant stimuli play an important role in the lives of insects, especially in the location of mating partners and oviposition sites, and the identification of food substances. They are detected by olfactory receptor cells borne by the antennae. These bipolar neurons are housed in sensilla, which are modified regions of cuticle with a diversity of forms and structural adaptations (see reviews of Altner and Prillinger 1980; Steinbrecht 1999). Typically, the external part of the sensillum is in the form of a hair with multiple tiny pores in the hair wall. The hair lumen is filled with a sensillum fluid which bathes the sensory dendrites and is isolated from the hemolymph filling the antennal lumen. Below the hair, the inner dendrite and soma of the neurons are ensheated in auxiliary cells that form specific parts of the sensillum during development (reviewed by Keil 1997). The odorant molecules penetrate within the hair through the pores and ultimately interact with receptor molecules borne by the dendritic membrane. Activation of these receptors triggers a transduction system which increases the membrane conductance (see e.g. Buck 1996; Schild and Restrepo 1998). A receptor potential develops and propagates passively to the initial segment of the axon where it triggers action potentials that are conducted to the brain (Hildebrand and Shepherd 1997). One of the most common techniques to record these electrical events from a sensillum consists of slipping a pipette filled with a saline solution over the cut end of the hair (Kaissling 1995; see also Hodgson et al. 1955). This pipette is used as the recording electrode, whereas the indifferent electrode is located in the hemolymph of the antennal cavity.

The first aim of this paper is to determine the equations that describe this experimental preparation. The whole system, including neuron, accessory cells and electrodes, is considered. We show how the difference in potential recorded between the tip of the hair sensillum and the hemolymph is related to the membrane potential at any point along the sensory dendrite and especially at the base of the dendrite. All signals received on the dendrite are integrated at the base, so that the potential there determines the potential on the rest of the non-sensory part of the neuron, including the action potential generator.

A. Vermeulen[1] · J.-P. Rospars (✉)[2]
Unité de Biométrie,
Institut National de la Recherche Agronomique,
78026 Versailles Cedex, France
E-mail: rospars@versailles.inra.fr
Tel.: +33-1-30833355; Fax: +33-1-30833359

Present addresses:
[1] Royal Netherlands Naval College,
1781 AC Den Helder, The Netherlands

[2]Unité de Phytopharmacie et Médiateurs Chimiques,
Institut National de la Recherche Agronomique,
78026 Versailles Cedex, France

The second aim is to generalize the description of the neuron itself. In a previous study (Vermeulen and Rospars 1998a) we analyzed two extreme models. The first one, called model A, is the classical model in which the whole neuron is assumed to be bathed in a homogeneous external medium, e.g. the hemolymph. A difference of concentration at rest is assumed between the internal and external media for the ion species that cross the membrane during stimulation. This gradient provides the driving force for the receptor current. On the contrary, in the second model, denoted B, the hemolymph bathes only the non-sensory part of the neuron (dendritic trunk, soma and axon). A sensillum lymph, of different ionic composition, bathes the sensory dendrite. Moreover, no gradient is assumed for the permeating ion, as suggested by experimental observations in insects (Kaissling and Thorson 1980; Thurm and Küppers 1980; Zufall and Hatt 1991). Consequently, the driving force for the receptor current is extradendritic, and arises in part from the gradient which is maintained by auxiliary cells between the sensillum lymph and the hemolymph. In the present paper these two extreme models are united in a single "mixed" model in which the driving force of the receptor current is provided both by the dendritic battery, as in model A, and the resting battery of the non-sensory part of the neuron plus an extraneuronal battery, as in model B. Of course, this mixed model is more general and adaptable than the extreme versions from which it is derived.

Our third aim is to analyze the steady-state responses of the insect olfactory neuron, that is model B, in this broader context. We show in particular how the tip-recorded receptor potential reflects its dendritic counterpart at the base of the sensory dendrite and how the steady-state response properties in magnitude, sensitivity and dynamic range deduced from the recorded potential reflect the dendritic response properties of the neuron. Finally, we also examine how these responses would be changed if the conditions defining model B were not strictly met but a measure of model A was introduced.

The presentation of the results is as follows: the tip-recorded potentials (first aim) are calculated in the first section. In order to calculate these potentials, the dendritic membrane and receptor potentials of the "mixed" model had to be calculated, which is done in the subsection entitled "Extracellular potential $V_e(x)$" (second aim). The comparison of both kinds of potentials and a brief study of their response properties are done in the second section (third aim).

Results

Determination of the tip-recorded potentials

The mixed model studied is shown in Fig. 1 with the same notations as in Vermeulen and Rospars (1998a); see Tables 1 and 2. For reasons of simplicity, we consider only a single sensory dendrite, although more dendrites can be easily included (see Discussion). Moreover, the non-sensory part of the neuron is not described in detail. It is replaced by its Thévenin equivalent, i.e. resistance R_{in} in series with battery E_{rN}. It can be shown that this part, with any shape and (passive) electrical properties, can be replaced by this simple circuit without loss in generality.

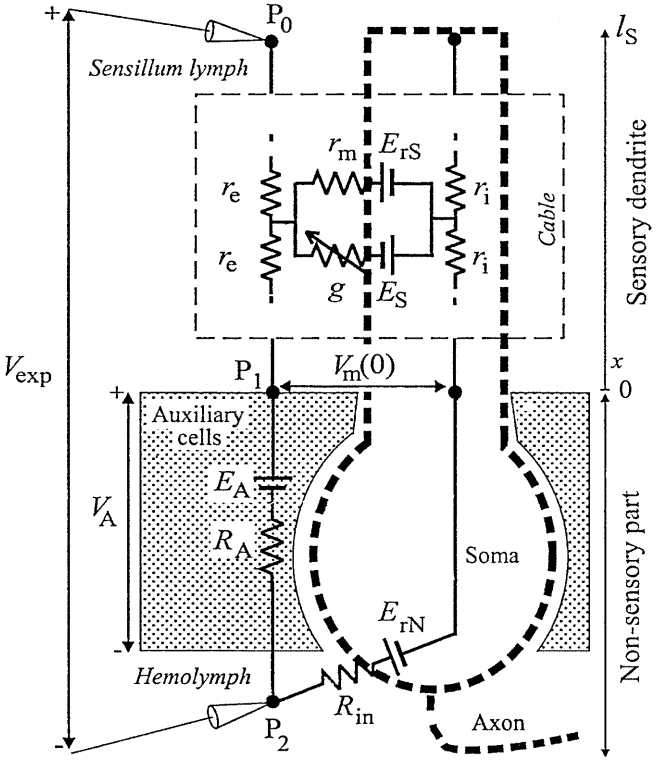

Fig. 1 Mixed model of the sensillum with neuron, auxiliary cells and recording electrodes. The neuron is composed of two parts connected at level P_1 (abscissa 0), a single sensory dendrite and a non-sensory part with dendritic trunk, soma and axon. The junction between auxiliary cells and the neuron, also at P_1, divides the extraneuronal space in two compartments, hemolymph and sensillum lymph, with different ionic compositions, which gives rise to the transepithelial battery E_A. The difference of concentrations of the permeating ion between the sensillum lymph and the intraneuronal medium gives rise to the sensory battery E_S. The membrane potentials are driven by E_A, E_S and two other batteries, E_{rS} and E_{rN}, which are the resting potentials in the sensory and non-sensory parts of the neuron, respectively. The potential V_{exp} is recorded between the tip of the dendrite and the hemolymph. All batteries are oriented in such a way that their electromotive forces (E_A, E_S, E_{rS}, E_{rN}) have positive values

Three basic kinds of potentials are considered at any point x along the sensory dendrite: the potentials inside $V_i(x)$ and outside $V_e(x)$ the neuron, and the membrane potential $V_m(x) = V_{rmi}(x) - V_e(x)$, and the receptor potential (depolarization) $\Delta V_m = V_m(x) - V_{m,r}(x)$, which is the difference between the membrane potential during stimulation and the membrane potential at rest. The transepithelial potential V_A is the extracellular potential $V_e(0)$ at point P_1 (see Fig. 1) of abscissa $x = 0$ at the base of the dendrite in the sensillum lymph. The tip-recorded potential V_{exp} is the extracellular potential $V_e(l_S)$ at the

Table 1 Symbols of parameters related to the morphology and electrical properties of the sensillum and its receptor neuron

Type	Symbol	Unit	Description
Morphology	X	cm	Abscissa along sensory dendrite
	P_0	–	Tip of sensory dendrite ($X=0$)
	P_1	–	Base of sensory dendrite ($X=L_S$)
	P_2	–	Axon initial segment (in hemolymph)
	L_S	cm	Length of dendrite
	D	cm	Diameter of dendrite
	D_e	cm	Diameter of extracellular space (hair lumen)
Electrical variables	R_i	Ω cm	Resistivity of intracellular medium of dendrite
	R_e	Ω cm	Resistivity of extracellular medium of dendrite
	R_m	Ω cm^2	Resistivity at rest across a unit area of dendritic membrane
	G_m	S cm^{-2}	Stimulation-dependent conductance per unit area of membrane
	E_S	mV	Reversal potential of permeating ions during stimulation
	E_{rS}	mV	Resting potential of dendrite
	E_{rN}	mV	Resting potential of non-sensory neuron segment
	E_A	mV	Battery simulating auxiliary cells
	R_A	Ω	Resistance simulating auxiliary cells
	R_{in}	Ω	Thévenin's input resistance of non-sensory neuron segment

Table 2 Definitions of derived variables related to resistances and potentials

Type	Definition	Unit	Description
Resistances	$r_m = R_m/\pi D$	Ω cm	Membrane resistance per unit length
	$g_m = G_m \pi D$	S cm^{-1}	Stimulation-dependent conductance per unit length
	$g = G_m/R_m{}^{-1} = r_m/g_m$	–	Dimensionless stimulation-dependent conductance
	$r_i = 4R_i/\pi D^2$	Ω W cm^{-1}	Resistance of intracellular medium per unit length
	$r_e = 4R_e/\pi(D_e{}^2 - D^2)$	Ω W cm^{-1}	Resistance of extracellular medium per unit length
	$\lambda = \sqrt{r_m/(r_e + r_i)}$	cm	Space constant of membrane
	$l_S = L_S/\lambda,\ x = X/\lambda$	–	Electrotonic length of dendrite and electrotonic abscissa
	$r_t = r_e + r_i$	Ω cm^{-1}	Sum of axial resistances per unit length
	$R_t = (r_e + r_i)\lambda$	Ω	Sum of axial resistances per space constant
	$r_{in} = (R_{in} + R_A)/R_t$	–	Input resistance of non-sensory part as a ratio with R_t
	$a = R_A/(R_{in} + R_A)$	–	Ratio of R_A with total resistance of non-sensory part
Potentials	$V_i(x),\ V_e(x)$	mV	Intra- and extracellular dendritic potentials at abscissa x
	$V_A = V_e(0)$	mV	Transepithelial potential
	$V_m(x) = V_i(x) - V_e(x)$	mV	Dendritic membrane potential at abscissa x during stimulation
	$V_{m,r}(x)$	mV	Resting dendritic membrane potential at x (no stimulation)
	$\Delta V_m(x) = V_m(x) - V_{m,r}(x)$	mV	Dendritic receptor potential at abscissa x
	$\Delta V_{m,M}(x)$	mV	Maximum dendritic receptor potential during stimulation at x
	$V^*(x) = \Delta V_m(x)/\Delta V_{m,M}(x)$	–	Relative receptor potential at abscissa x
	$V_{exp} = V_e(l_S)$	mV	Tip-recorded potential at point P_0 (tip)
	$\Delta V_{exp} = V_{exp} - V_{exp,r}$	mV	Tip-recorded receptor potential at point P_0

tip (point P_0) of the dendrite. Actually, all these potentials are differences of potentials with respect to the potential at point P_2 in the hemolymph, which can be considered as potential zero.

All these potentials are calculated first at point P_1 using the Thévenin's equivalent (next subsection), then their variation along the dendrite between P_1 and P_0 using the cable equation (following subsection). Finally, these two contributions are summed to obtain the tip-recorded potential at point P_0 (last subsection). Continuous spatial changes of potentials are considered along the line P_0P_1 only.

Potentials at the base of the sensory dendrite in situ

Transepithelial potential V_A

To determine the transepithelial potential V_A, the electrical circuit of Fig. 1 can be simplified by using the

Thévenin's equivalent circuit of the sensory dendrite. Under steady-state conditions this circuit, which consists of a resistance R_{TS} in series with a battery E_{TS} (Fig. 2), is strictly equivalent to that of Fig. 1. It can be shown (Vermeulen and Rospars 1998a, 1998b) that for a uniformly stimulated dendrite the resistance (called input resistance of the sensory dendrite) is:

$$R_{TS} = \frac{R_t}{\sqrt{1+g}} \coth\left(\sqrt{1+g}\, l_S\right) \tag{1}$$

and the battery is:

$$E_{TS} = \frac{gE_S - E_{rS}}{1+g} \tag{2}$$

The circuit obtained contains only one loop. The current I circulating in this loop is given by Ohm's law:

$$I = \frac{\sum E}{\sum R} = \frac{E_{rN} + E_A + E_{TS}}{R_{in} + R_A + R_{TS}} \tag{3}$$

which, after replacement of R_{TS} and E_{TS} by their expressions (1) and (2) is:

$$I = \frac{(1+g)(E_{rN}+E_A) + gE_S - E_{rS}}{(1+g)(R_{in}+R_A) + \sqrt{1+g}R_t \coth(\sqrt{1+g}\, l_S)} \tag{4}$$

As can been seen in Fig. 2, the transepithelial potential is given by $V_A = E_A - IR_A$, which can be written as

$$V_A = E_A - \frac{(1+g)(E_{rN}+E_A) + gE_S - E_{rS}}{(1+g)r_{in} + \sqrt{1+g}\coth(\sqrt{1+g}\, l_S)} a r_{in} \tag{5}$$

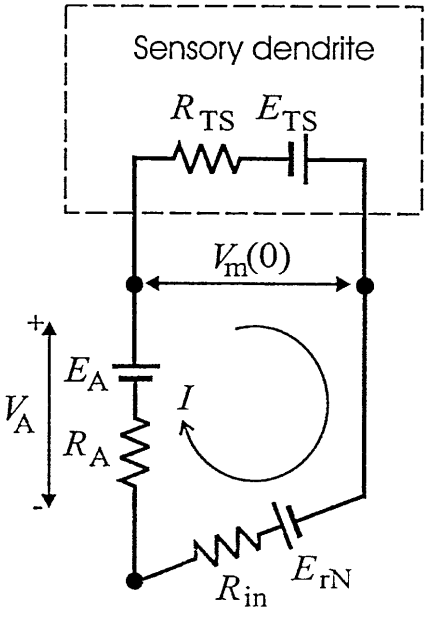

Fig. 2 Simple circuit of the sensillum shown in Fig. 1 for determining the epithelial potential E_A and the membrane potential $V_m(0)$ at level P_1. The neuron and its environment are replaced by three Thévenin's circuits equivalent to the sensory dendrite (R_{TS} and E_{TS}), the non-sensory part of the neuron (R_{in} and E_{rN}) and the auxiliary cells (R_A and E_A)

where r_{in} is the dimensionless input resistance of the non-sensory part, $r_{in} = (R_{in} + R_A)/R_t$ (see also Vermeulen and Rospars 1998a), and a is the ratio of the transepithelial resistance to the total resistance R_{TN} of the non-sensory part, $a = R_A/(R_{in} + R_A)$.

Membrane and receptor potentials at the base P_1 of the dendrite

Similarly, the membrane potential at the base of the sensory dendrite (abscissa $x = 0$) is $V_m(0) = E_{TS} - IR_{TS}$, which is

$$V_m(0) = \frac{1}{1+g}\left(gE_S - E_{rS} - \frac{(1+g)(E_{rN}+E_A) + gE_S - E_{rS}}{\sqrt{1+g}\, r_{in}\tanh(\sqrt{1+g}\, l_S) + 1}\right) \tag{6}$$

This equation is a generalization of Eqs. 9 and 10 in Vermeulen and Rospars (1998a). Taking $E_A = 0$ and $E_{rS} = E_{rN} = E_r$ gives the special case of the autonomous neuron (model A), whereas taking $E_S = E_{rS} = 0$ gives the other extreme case of the neuron that depends on auxiliary cells (model B).

In general, the value of the membrane potential is not in itself the quantity of interest. More meaningful is its change as a function of the stimulus intensity, which is the receptor potential. At any given point x of the neuron membrane, the receptor potential $\Delta V_m(x)$ is defined as the membrane potential (or depolarization) $V_m(x)$ for a given value of the stimulation-dependent conductance g, with respect to the depolarization $V_{m,r}(x)$ at rest in the absence of stimulation, $g = 0$. In the present case, one obtains:

$$\Delta V_m(0) = V_m(0) - V_{m,r}(0) \tag{7}$$

where $V_m(0)$ and $V_{m,r}(0)$ are given by Eq. (6), with:

$$V_{m,r}(0) = \frac{E_{rS} - (E_{rN}+E_A)}{r_{in}\tanh(l_S) + 1} - E_{rS} \tag{8}$$

The maximum value of the receptor potential $\Delta V_m(0)$ for a strong stimulation g is:

$$\Delta V_{m,M}(0) = E_S + \frac{E_{rN}+E_A}{r_{in}\tanh(l_S)+1} + \frac{E_{rS}}{r_{in}\tanh(l_S)+1} r_{in}\tanh(l_S) \tag{9}$$

It depends linearly on the e.m.f. of the batteries.

Potentials along the isolated sensory dendrite

In this section the membrane $V_m(x)$ and extracellular $V_e(x)$ potentials are calculated as a function of the distance x along the dendrite, under the following conditions. (1) The sensory dendrite is considered in isolation, as if severed from the rest of the neuron, so that the

extracellular potential at the base of the dendrite is zero, $V_e(0)=0$; see Fig. 3A (in the next section this isolated dendrite will be included in the sensillum model). (2) The membrane potential at the base of the sensory dendrite is clamped at a given potential, $V_m(0)$. (3) The distal end of the dendrite is sealed (no current leak).

Membrane potential $V_m(x)$

The membrane potential $V_m(x)$ can be calculated from the cable equation. The dimensionless form of this second-order ordinary differential equation is:

$$V_m''(x) - (1+g)V_m(x) + gE_S - E_{rS} = 0 \tag{10}$$

for $0 \geq x \geq l_S$, where x is the distance from the base of the dendrite expressed in membrane space constants, and $'$ means differentiation with respect to x; see Appendix A. As shown in Appendix B, the solution of Eq. (10) is

$$V_m(x) = \left(\cosh\left(\sqrt{1+g}x\right) - \tanh\left(\sqrt{1+g}l_S\right)\sinh\left(\sqrt{1+g}x\right)\right) \times \left(V_m(0) - \frac{gE_S - E_{rS}}{1+g}\right) + \frac{gE_S - E_{rS}}{1+g}, \quad \text{for } 0 \geq x \geq l_S \tag{11}$$

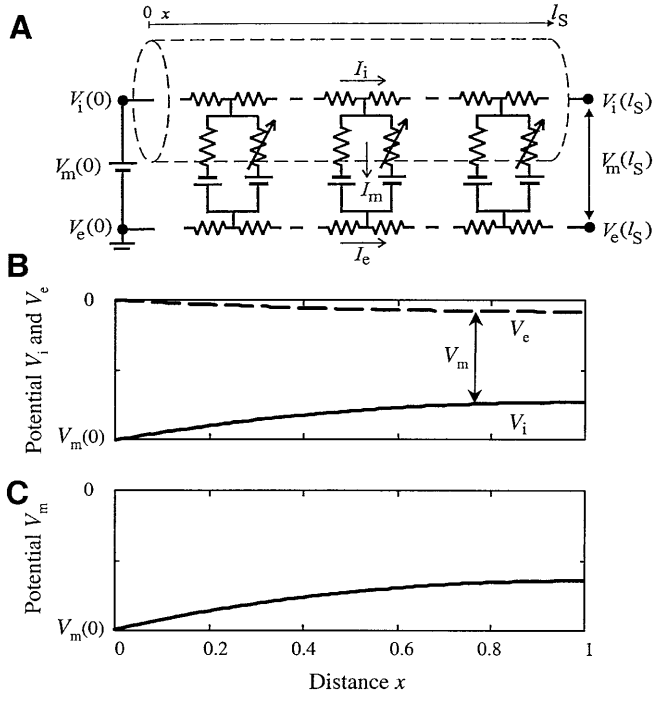

Fig. 3 Potentials along the sensory dendrite (distance x expressed in membrane space constants) represented by a one-dimensional cable (**A**), with $V_i(x)$ and $V_e(x)$ potentials of the intra- (*dashed*) and extracellular (*solid*) media, respectively (**B**), and $V_m(x)$ membrane potential (**C**). Parameters: $l_S=1$, $g=0$, $E_{rS}=0$, $E_S=0$, $r_e/r_i=0.3$

Extracellular potential $V_e(x)$

As shown in Appendix C, the spatial distribution of the extracellular potential is:

$$V_e(x) = \frac{r_e}{r_e + r_i}\left(V_m(0) - V_m(x)\right) \tag{12}$$

This relation can be understood intuitively. It shows that the decrease of the membrane potential along the dendrite ($V_m(0) - V_m(x)$) is divided over the intra- and extracellular spaces according to the values of the axial resistances r_i and r_e, respectively. This is also illustrated in Fig. 3B and C.

Tip-recorded potentials

The potential V_{exp} recorded at the tip of the hair by an electrode slipped on it is the sum of two terms calculated in the previous sections: (1) the transepithelial potential V_A, which is equal to the extracellular potential at the base P_1 of the dendrite $V_e(0)$, and (2) the difference between the extracellular potentials at the tip P_0 and at the base P_1 of the sensory dendrite, $V_e(l_S) - V_e(0)$:

$$V_{exp} = V_A + \left(V_e(l_S) - V_e(0)\right) \tag{13}$$

Using Eq. (12) one obtains:

$$V_{exp} = V_A + \frac{r_e}{r_e + r_i}\left(V_m(0) - V_m(l_S)\right) \tag{14}$$

Using Eq. (11) and $\cosh^2 - \sinh^2 = 1$, the membrane potential at the tip of the dendrite $V_m(l_S)$ can be written:

$$V_m(l_S) = \frac{V_m(0)}{\cosh(\sqrt{1+g}l_S)} + \frac{gE_S - E_{rS}}{1+g}\left(1 - \frac{1}{\cosh(\sqrt{1+g}l_S)}\right) \tag{15}$$

so that:

$$V_{exp} = V_A + \frac{r_e}{r_e + r_i}\left(V_{rmm}(0) - \frac{gE_S - E_{rS}}{1+g}\right) \times \left(1 - \frac{1}{\cosh(\sqrt{1+g}l_S)}\right) \tag{16}$$

where the transepithelial potential V_A is given by Eq. (5), and the membrane potential at the base of the dendrite $V_m(0)$ by Eq. (6). Potential V_{exp} resulting from all these terms is a long but straightforward equation which need not be given explicitly here. The resting value $V_{exp,r}$ of the tip-recorded potential for $g=0$ is easily derived from Eqs. (16), (5) and (8), as:

$$V_{exp,r} = E_A + \frac{E_{rS} - (E_{rN} + E_A)}{r_{in}\tanh(l_S) + 1} \times \left(ar_{in}\tanh(l_S) + \frac{r_e}{r_e + r_i}\left(1 - \frac{1}{\cosh(l_S)}\right)\right) \tag{17}$$

By analogy with Eq. (7) one can define the tip-recorded receptor potential ΔV_{exp} as:

$$\Delta V_{\mathrm{exp}} = V_{\mathrm{exp}} - V_{\mathrm{exp,r}} \tag{18}$$

where V_{exp} is given by Eq. (16) and $V_{\mathrm{exp,r}}$ by Eq. (17). The asymptotic value of $V_{\mathrm{exp}}(g \to \infty)$ is:

$$\Delta V_{\mathrm{exp,M}} = -aE_{\mathrm{S}} + \frac{E_{\mathrm{rN}} + E_{\mathrm{A}}}{r_{\mathrm{in}} tanh(l_{\mathrm{S}}) + 1}\left(\frac{r_{\mathrm{e}}}{r_{\mathrm{e}} + r_{\mathrm{i}}}\left(1 - \frac{1}{\cosh(l_{\mathrm{S}})}\right) - a\right) - \frac{E_{\mathrm{rS}}}{r_{\mathrm{in}} \tanh(l_{\mathrm{S}}) + 1}\left(\frac{r_{\mathrm{e}}}{r_{\mathrm{e}} + r_{\mathrm{i}}}\left(1 - \frac{1}{\cosh(l_{\mathrm{S}})}\right) - a r_{\mathrm{in}} \tanh(l_{\mathrm{S}})\right). \tag{19}$$

This equation shows that $\Delta V_{\mathrm{exp,M}}$, like its counterpart $\Delta V_{\mathrm{m,M}}(0)$ (see Eq. 9), depends linearly on the e.m.f. of the batteries.

Special case of model B

It has been suggested (Kaissling and Thorson 1980) that, in the insect sex-pheromone receptor neuron, no batteries are located in the membrane of the sensory dendrite, so $E_{\mathrm{rS}} = 0$ and $E_{\mathrm{S}} = 0$. Under the condition $E_{\mathrm{rS}} = E_{\mathrm{S}} = 0$, Eq. (16) simplifies to:

$$V_{\mathrm{exp}} = E_{\mathrm{A}} - \frac{E_{\mathrm{rN}} + E_{\mathrm{A}}}{\sqrt{1+g} r_{\mathrm{in}} \tanh(\sqrt{1+g} l_{\mathrm{S}}) + 1} \times \left(\sqrt{1+g} a r_{\mathrm{in}} \tanh\left(\sqrt{1+g} l_{\mathrm{S}}\right) + \frac{r_{\mathrm{e}}}{r_{\mathrm{e}} + r_{\mathrm{i}}}\left(1 - \frac{1}{\cosh(\sqrt{1+g} l_{\mathrm{S}})}\right)\right) \tag{20}$$

The tip-recorded receptor potential ΔV_{exp} can be calculated from Eq. (18). This is a relatively long equation. However, the expression of its asymptotic value obtained for large stimulations ($g \to \infty$) is short:

$$\Delta V_{\mathrm{exp,M}} = \frac{E_{\mathrm{rN}} + E_{\mathrm{A}}}{r_{\mathrm{in}} \tanh(l_{\mathrm{S}}) + 1}\left(\frac{r_{\mathrm{e}}}{r_{\mathrm{e}} + r_{\mathrm{i}}}\left(1 - \frac{1}{\cosh(l_{\mathrm{S}})}\right) - a\right) \tag{21}$$

In Eq. (21) it can be seen that the maximum amplitude $\Delta V_{\mathrm{exp,M}}$ decreases when the extracellular medium is not isopotential. It is also worth mentioning that the relative receptor potentials $V^*_{\mathrm{m}}(0) = \Delta V_{\mathrm{m}}(0)/\Delta V_{\mathrm{m,M}}(0)$ and; $V^*_{\mathrm{exp}} = \Delta V_{\mathrm{exp}}/\Delta V_{\mathrm{exp,M}}$ do not depend on any battery. This is also the case of the ratio of the dendritic and tip-recorded receptor potentials:

$$\frac{\Delta V_{\mathrm{exp,M}}}{\Delta V_{\mathrm{m,M}}(0)} = \frac{r_{\mathrm{e}}}{r_{\mathrm{e}} + r_{\mathrm{i}}}\left(1 - \frac{1}{\cosh(l_{\mathrm{S}})}\right) - a \tag{22}$$

Comparison of the dendritic and tip-recorded responses

In this section the dendritic membrane $V_{\mathrm{m}}(0)$ and receptor potentials $\Delta V_{\mathrm{m}}(0)$ at point P_1, which integrate the dendritic contribution before it is converted to action potentials, are compared to their tip-recorded counterparts V_{exp} and ΔV_{exp} at point P_0. The base P_1 of the dendrite owes its special importance to the fact that the receptor potential along the non-sensory part of the neuron is everywhere proportional to its value $\Delta V_{\mathrm{m}}(0)$ at P_1, as shown in a previous work (Vermeulen and Rospars 1998a). This is why we can limit our attention to the dendritic potentials defined at this level.

The dendritic and tip-recorded values of the receptor potential and of the characteristics of the conductance-potential curves were compared for several values of the parameters ($r_{\mathrm{e}}/r_{\mathrm{i}}$, a, r_{in}, l_{S} and values of the batteries). Of special importance in this comparison are the parameters $r_{\mathrm{e}}/r_{\mathrm{i}}$ and a, which express the non-isopotential character of the sensillum lymph and the resistance between the sensillum and hemolymph, respectively, both of which are new to this study. The central values were chosen close to those estimated in the moth *Antheraea polyphemus* (Kaissling 1987; Kodadová and Kaissling 1996). For each parameter, smaller and larger values were also tried. The following conclusions apply to this subset of the parameter space.

Comparison of the dendritic and tip-recorded potentials

The dendritic membrane potential and the tip-recorded potential are of opposite signs, $V_{\mathrm{m}}(0) < 0$ and $V_{\mathrm{exp}} > 0$ (Fig. 4, top row). Moreover, the receptor potentials are also of opposite signs, i.e. $\Delta V_{\mathrm{m}}(0) > 0$ and $\Delta V_{\mathrm{exp}} < 0$ (Fig. 4, middle row). The negative depolarization ΔV_{exp} is in agreement with observations (see e.g. fig. 29 in Kaissling 1987). The positive value of the receptor potential at the initial segment is in agreement with the expectation that a greater stimulation evokes a greater receptor potential that in turn elicits a higher firing rate.

The dendritic receptor potential is always a sigmoid function of the conductance g at the sensory membrane. This is also usually the case of the tip-recorded receptor potential. In this typical situation, shown in Fig. 4 (left column, solid line), maximum values and asymptotic values for $g \to \infty$ are equal. However, for some (atypical) values of the parameters, non-sigmoid curves are found (see Fig. 4, dashed line, and Fig. 5). These non-sigmoid experimental curves appear only for certain combinations of the values of the ratios r_e/r_i and a, see Fig. 5. As shown on top of this figure, two types of non-sigmoid curves can be observed: one with a negative and the other with a positive "overshoot". The location of the border between these two kinds of curves seems to be mainly determined by the dendritic length l_{S}; for small values of l_{S} the border is close to the vertical axis, and for larger values it is shifted towards the border between sigmoid and non-sigmoid curves. However, for large values of the dendritic length ($l_{\mathrm{S}} > 5$), the curves are again of a sigmoid shape. The batteries and the input resistance in the range 0.1–1.0 have a minor influence on the appearance of the non-sigmoid curves.

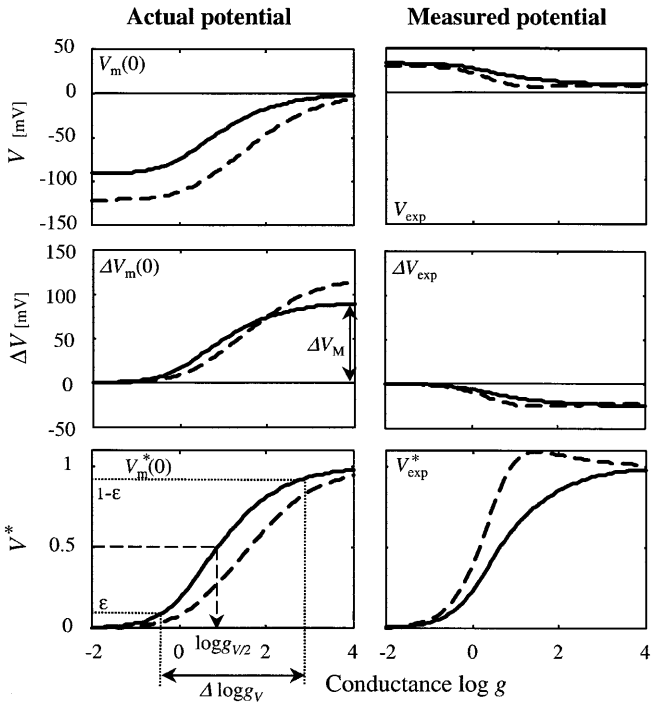

Fig. 4 Dendritic and tip-recorded potentials as a function of the sensory conductance g. *Top row*: dendritic membrane potential $V_m(0)$, Eq. (11), at the base of sensory dendrite (level P_1) and experimentally tip-recorded potential V_{exp}, Eq. (20), at the tip of the dendrite (level P_0). *Middle row*: dendritic receptor potential $\Delta V_m(0)$ at P_1 and tip-recorded receptor potential ΔV_{exp} at P_0, Eq. (18). *Bottom row*: relative potentials $V_m^*(0) = \Delta V_m(0)/\Delta V_{m,M}(0)$ and $V_{exp}^* = \Delta V_{exp}/\Delta V_{exp,M}$ (see Eqs. 18 and 19), with the three response properties (see text) shown on the left. Parameters: $r_e/r_i = 0.1$, $r_{in} = 0.7$ (*solid line*), $r_e/r_i = 0.5$, $r_{in} = 0.2$ (*dashed line*), $a = 0.3$, $l_S = 1$, $E_{rS} = 0$, $E_S = 0$, $E_{rN} = 90$ mV, $E_A = 50$ mV

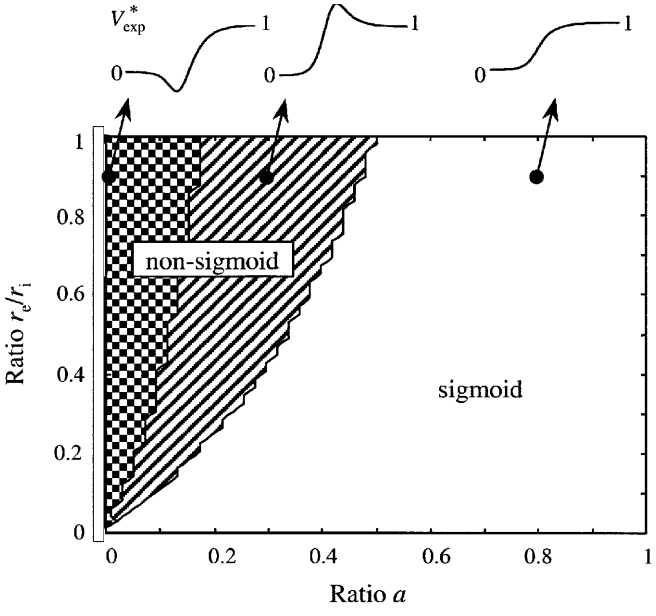

Fig. 5 Shape of the conductance-response curves for various combinations of the parameters r_e/r_i and a (see Table 2). The conductance-response curves are the tip-recorded receptor potential ΔV_{exp} versus log g, or equivalently relative value $V_{exp}^* = \Delta V_{exp}/\Delta V_{exp,M}$ versus log g, as shown in Fig. 4. Depending on the parameter values the curves can be sigmoid, non-sigmoid with right overshoot or non-sigmoid with left undershoot. Parameters: $r_{in} = 0.7$, $l_S = 1$, $E_{rS} = 0$, $E_S = 0$, $E_{rN} = 90$ mV, $E_A = 50$ mV

Comparison of the dendritic and tip-recorded response properties

The response properties (maximum response along the ΔV-axis, sensitivity and dynamic range along the g-axis; see also Fig. 4, left column) are defined only for sigmoid curves. The exceptional case of non-sigmoid curves is not considered here.

The *maximum* value (ΔV_M) of the dendritic receptor potential $\Delta V_m(0)$ is independent of a and r_e/r_i (see Fig. 6), decreases with r_{in} and l_S, and increases linearly with the e.m.f of the batteries (E_A, E_S, E_{rS}, E_{rN}). It is always greater than the tip-recorded maximum. In the special case $E_S = E_{rS} = 0$ (model B), Eq. (22) shows that the ratio tip-recorded/dendritic for maximum receptor potentials is independent of the batteries. The tip-recorded receptor potential computed with the standard values of the parameters (24 mV) is close to that found experimentally (about 30 mV; see table 1 in Kaissling 1987).

The *sensitivity* of the sigmoid conductance-potential curves can be characterized by the conductance at half-maximum response ($g_{V/2}$). Depending on the value of the parameters, this conductance $g_{V/2}$ for the dendritic receptor potential is 10–100 times greater than the membrane conductance at rest. It is independent of E_A, E_{rN}, r_e/r_i and a, only weakly dependent on E_S and E_{rS}, and increases with l_S and r_{in} (the dependence on the latter two parameters was discussed in detail for model B in Vermeulen and Rospars 1998a). The sensitivity of the tip-recorded receptor potential is always smaller or equal than that of its dendritic counterpart. This means that the dendritic sensitivity can be higher than the experimentally observed one. The tip-recorded sensitivity behaves like the dendritic one, except that it increases with r_e/r_i and decreases with a (see Fig. 6). The increase with r_e/r_i is smaller for shorter dendrites and ceases beyond a point where the curve is no longer sigmoid. In the special case $r_e/r_i = 0$, which corresponds to an isopotential sensillum lymph, the curves of the relative receptor potentials V^*, i.e. the ratio of the receptor potential at any conductance to its maximum value, are identical for the dendritic and the tip-recorded receptor potentials. It follows of course that their sensivities are the same.

The *dynamic range* ($\Delta \log g_V$) of the dendritic conductance-potential curves estimated with $\varepsilon = 5\%$ (see definition in Fig. 4) is usually close to 4 log units. It is independent of r_e/r_i, a, E_A and E_{rN}, only weakly dependent on E_S and E_{rS}, increases with l_S and decreases with r_{in} (see Vermeulen and Rospars 1998a). The dynamic ranges of the tip-recorded sigmoid curves are smaller than those of the corresponding dendritic curves, except with some parameter values for which a very slight increase can be observed (for example, observed 4.12 instead of dendritic 3.92 at $r_e/r_i = 0.3$, $a = 0.3$, $l_S = 3$,

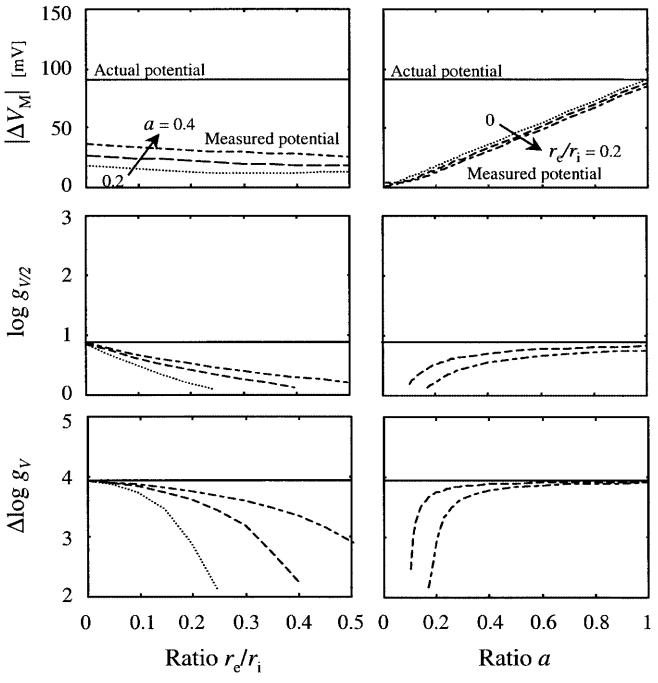

Fig. 6 Comparison of the response properties of the dendritic $\Delta V_m(0)$ (*solid line*) and tip-recorded ΔV_{exp} (*other lines*) receptor potentials as functions of the ratio r_e/r_i of the resistances of the external and internal media (*left column*) and the ratio $a = R_A/(R_{in} + R_A)$ of the transepithelial resistance to the total resistance of the non-sensory part (*right column*). *Top row*: absolute value of maximum response $|\Delta V_M|$; *middle row*: conductance at half-maximum response log $g_{V/2}$; *bottom row*: dynamic range Δlog g_V. Curves are interrupted for non-sigmoidal responses. Parameters: $r_{in} = 0.7$, $l_S = 1$, $E_{rS} = 0$, $E_S = 0$, $E_{rN} = 90$ mV, $E_A = 50$ mV; on left side, $a = 0.2$ (*dotted*, falls in middle and bottom row together with solid line), 0.3 (*dashed*), 0.4 (*dash-dotted*); on right side $r_e/r_i = 0$ (*dotted*), 0.1 (*dashed*), 0.2 (*dash-dotted*)

with standard values for the other parameters). The difference increases under the same conditions as those reported above for the sensitivity. Under certain values of a and above certain values of r_e/r_i, the tip-recorded dynamic ranges fall abruptly. Finally, in the case of the isopotential sensillum lymph, the dendritic and tip-recorded dynamic ranges are the same.

The newly introduced parameters r_e/r_i and a influence primarily the difference between the dendritic and tip-recorded response properties. Among the other parameters (l, r_{in}, E_A, E_S, E_{rS}, E_{rN}), the most influential on this difference is l_S. This is consistent with the special case illustrated by Eq. (22), in which a plays a major role.

Discussion

In the present work, analytical expressions are derived for the dendritic and the tip-recorded steady-state receptor potentials of a sensory neuron at rest and under constant stimulation. The study considers primarily an insect olfactory sensillum, although the results obtained can be applied to any kind of arthropod chemosensory sensillum. The recording electrode is considered to be slipped over the tip of the sensillum, which is a classical procedure for in situ recordings of these types of sensilla. For most values of the parameters the tip-recorded conductance-voltage curves are qualitatively similar to their dendritic counterparts, i.e. both are monotonously increasing sigmoidal curves. However, for some values (see Fig. 5) the tip-recorded curve presents either negative values or a maximum and then levels off to its asymptotic level. These deviations from the sigmoid shape are never observed for dendritic conductance-voltage curves.

One of the originalities of the biophysical model proposed is that it integrates two extreme neuron models, which up to now were studied separately. The first model is the classical model of the neuron bathing in a homogeneous environment (e.g. Rospars et al 1996; called model A in Vermeulen and Rospars 1998a), in which the driving force for the receptor potential comes from the ionic gradient between the internal and external sides of the sensory dendrite. In the second model (e.g. Kaissling and Thorson 1980; Kodadová and Kaissling 1996; called model B in Vermeulen en Rospars 1998a), the driving force comes from the ionic gradient developed by auxiliary cells surrounding the neuron between the hemolymph and the sensillum lymph. In the "mixed" model presented here the driving force comes from both the neuron and the auxiliary cells. This generalizes the previous models and gives the opportunity of studying the response properties of the neuron in a broader context.

In the case of the insect sex-pheromone receptor cell, the assumption of the absence of batteries in the sensory dendrite, which characterizes model B, is based on patch clamp observations for the reversal potential (Zufall and Hatt 1991) and on a particularly high potassium concentration in the sensillum lymph for the resting potential (Kaissling and Thorson 1980). This is the reason why all numerical illustrations shown are based on this assumption. In this model the ratio of the tip-recorded receptor potential to its maximum value under strong stimulation is independent of the values of the batteries and depends only on the values of the resistances. We show that the same result is also true for the dendritic receptor potential and for the ratio tip-recorded/dendritic of the maximum receptor potentials. With estimated values of the parameters (Kaissling and Thorson 1980; Kaissling 1987; Fig. 4, solid line) the latter ratio is −0.27, i.e. the tip-recorded maximum receptor potential is only about one fourth of the dendritic one, and of opposite sign. We show that the parameters that most influence the difference between the dendritic and tip-recorded voltages are the ratio r_e/r_i of the resistances per unit length of the sensillum lymph and the intradendritic medium, the ratio a of the auxiliary-cell resistance to the total resistance of the nonsensory part, and the length l_S of the dendrite.

However, it cannot be excluded that the dendritic batteries E_S and E_{rS} are actually small instead of zero. Calculations with the "mixed" model show that the

maximum values of the dendritic and tip-recorded receptor potentials depend linearly on the values of the batteries, but that their effect on the sensitivity and dynamic range are small. It follows that the conclusions drawn from Model B with no batteries in the sensory dendrite remain applicable when the dendrite contains batteries with relatively small values. This conclusion could also be drawn from numerical (discrete) models as used by Kaissling and Thorson (1980) and Kodadová and Kaissling (1996). However, the analytical solutions given here allow a better insight into the role of the various parameters of the model.

The model presented can be generalized to other neuron types. In particular, it can easily be extended to take more than one sensory dendrite into account. This can be done by replacing the input resistance r_{in} in all equations by the product Nr_{in}, where N is the number of sensory dendrites. This property has been mentioned previously (Vermeulen and Rospars 1998a) and is also true here because multiplying the number of sensory dendrites by N always divides the input resistance R_{TS} by N. This corresponds to a multiplication of r_{in} by N [see Eq. (3) and the definition of r_{in}].

The main limitations of the model presented are its lack of time-dependent aspects; it cannot mimic transient responses to the odorant stimulus or experimentally applied current/voltage steps, and it does not generate spikes (no active membrane properties are incorporated). These shortcomings can only be overcome by using a numerical model, although not all relevant parameters of the insect olfactory sensillum are known, in particular the electrical membrane properties and their spatial distribution within the sensillum. Hence more experimental work in the line of, for example, Kaissling and Thorson (1980), de Kramer (1985), Redkozubov (1995), Kodadová and Kaissling (1996) and Zufall and Hatt (1991), is essential. In the meantime, a more modest approach, based on simplified analytical models as used by de Kramer et al (1984) or Redkozubov (1995), remains useful for modeling simple transient responses.

Appendix

A. Cable equation and extracellular potential

The cable equation (see for example Tuckwell 1988) is derived by bringing together four features of the electrical circuit describing a uniform cable in a non-isopotential extracellular medium (see Fig. 3A and Tables 1 and 2 for a precise definition of resistances, conductances and batteries): First, the change in intra- and extracellular potentials is described by Ohm's law, $V_i'(X) = r_i I_i(X)$ and $V_e'(X) = r_e I_e(X)$, respectively. Here $I_i(X)$ and $I_e(X)$ are the axial currents in the intra- and extracellular media, r_i and r_e are the axial resistances in these media and X is a point along the cable at a distance expressed in centimetres from the base of the dendrite. Second, the cable is leaky so that a current $I_m(X)$ flows through the membrane. This current is equal to the change of the axial currents, $I_i'(X) = -I_m(X)$and $I_e'(X) = I_m(X)$. These two features can also be written as a system of coupled differential equations:

$$V_m''(X) = r_i I_m(X)$$
$$V_e''(X) = -r_e I_m(X) \quad \text{(A1)}$$

Third, the membrane current I_m(X) flows through the electrical circuit describing a path of the membrane:

$$I_m(X) = \frac{1}{r_m}(V_i(X) - (V_e(X) + E_{rS}) + g(V_i(X) - (V_e(X) + E_S))) \quad \text{(A2)}$$

Fourth, the membrane potential is defined as the difference of potential between the intra- and extracellular media, $V_m(X) = V_i(X) - V_e(X)$. This relation holds also for the second derivative of these potentials, $V_m''(X) = V_i''(X) - V_e''(X)$ so from this relation and Eq. (A1), one obtains:

$$V_m''(X) = r_i I_m(X) - (-r_e I_m(X)) = (r_i + r_e) I_m(X) \quad \text{(A3)}$$

Finally, the cable equation (Eq. 10) is obtained from the combination of Eqs. (A2) and (A3) and by expressing the distance along the sensory dendrite in units of the membrane space constant $\lambda = \sqrt{r_m/(r_i + r_e)}$ (see Table 2) so that $x = X/\lambda$. Furthermore, the relation between the extracellular and membrane potentials is obtained from Eqs. (A1) and (A3) with $x = X/\lambda$:

$$V_e''(x) = -\frac{r_e}{r_e + r_i} V_m''(x) \quad \text{(A4)}$$

It is interesting to note that Eq. (A4) is independent of the membrane current. Therefore, it is valid also when additional terms are added to Eq. (A2), for example the membrane capacitive current in the non-stationary case, a current injected by the experimenter or a synaptic current.

B. Membrane potential

The cable equation (Eq. 10) is an ordinary second-order differential equation. Its general solution is the sum of the particular solution $V_p(=(gE_S - E_{rS})/(1+g))$ and the solution V_h of the homogenous equation. This homogenous equation is given by Eq. (10) with $E_{rS} = E_S = 0$ and its general solution is $V_h(x) = A\sinh(\sqrt{1+g}x) + B\cosh(\sqrt{1+g}x)$. Hence the membrane potential is given by:

$$V_m(x) = A\sinh\left(\sqrt{1+g}x\right) + B\cosh\left(\sqrt{1+g}x\right) + \frac{gE_S - E_{rS}}{1+g} \quad \text{(B1)}$$

for $0 \geq x \geq l$, where the constants A and B have to be calculated from the boundary conditions: (1) a sealed distal end, $V_m'(l) = 0$, and (2) a clamped potential at the base of the dendrite ($V_m(0)$). Taking into account that $V_m'(x) = \sqrt{1+g}(A\cosh(\sqrt{1+g}x) + B\sinh(\sqrt{1+g}x))$, one finds:

$$A = -\left(E_c - \frac{gE_S - E_{rS}}{1+g}\right)\tanh\left(\sqrt{1+g}l_S\right) \quad \text{(B2)}$$

and:

$$B = V_m(0) - \frac{gE_S - E_{rS}}{1+g} \quad \text{(B3)}$$

Equation (11) is obtained from the combination of Eqs. (B1), (B2) and (B3).

C. Extracellular potential

The spatial distribution of the extracellular potential $V_e(x)$ is rarely calculated because the external medium is generally considered as

isopotential. In Appendix A this quantity is used in the derivation of the cable equation. The relation between the extracellular potential and the membrane potential is given by Eq. (A4). After integrating once in x, Eq. (A4) becomes:

$$V_e'(x) = -\frac{r_e}{r_e + r_i} V_m'(x) + A \tag{C1}$$

where A is a constant which depends on the boundary conditions. From the sealed-end condition at the tip of the dendrite, $V_e'(l_S) = V_m'(l_S) = 0$, one obtains $A = 0$. Integrating a second time gives the extracellular potential:

$$V_e(x) = -\frac{r_e}{r_e + r_i} V_m(x) + B \tag{C2}$$

Using the second boundary condition, $V_e(0) = 0$, permits one to determine constant B: $B = r_e V_m(0)/(r_e + r_i)$.

References

Altner H, Prillinger L (1980) Ultrastructure of invertebrate chemo-, thermo-, and hygroreceptors and its functional significance. Int Rev Cytol 67: 69–139

Buck L (1996) Information coding in the vertebrate olfactory system. Annu Rev Neurosci 19: 517–544

Hildebrand JG, Shepherd GM (1997) Mechanisms of olfactory discrimination: converging evidence for common principles across phyla. Annu Rev Neurosci 20: 595–631

Hodgson ES, Lettvin JY, Roeder KD (1955) Physiology of a primary chemoreceptor unit. Science 122: 417–418

Kaissling K-E (1987) In: Colbow K (ed) RH Wright lectures on insect olfaction. Simon Fraser University, Burnaby BC, Canada

Kaissling K-E (1995) Single unit and electroantennogram recordings in insect olfactory organs. In: Spielman AI, Brand JG (eds) Experimental cell biology of taste and olfaction, current techniques and protocols. CRC Press, Boca Raton, pp 361–377

Kaissling K-E, Thorson J (1980) Insect olfactory sensilla: structural, chemical and electrical aspects of the functional organization. In: Satelle DB, Hall LM, Hildebrand JG (eds) Receptors for neurotransmitters, hormones and pheromones in insects. Elsevier, Amsterdam, pp 261–282

Keil TA (1997) Comparative morphology of sensillum development. Int J Insect Morphol Embryol 26: 151–160

Kodadová B, Kaissling K-E (1996) Effects of temperature on silkmoth olfactory responses to pheromone can be simulated by modulation of resting cell membrane resistances. J Comp Physiol A 179: 15–27

Kramer JJ de (1985) The electrical circuitry of an olfactory sensillum in *Antherea polyphemus*. J Neurosci 5: 2484–2493

Kramer JJ de, Kaissling K-E, Keil T (1984) Passive electrical properties of insect olfactory sensilla may produce the biphasic shape of spikes. Chem Senses 8: 289–295

Redkozubov A (1995) High electrical resistance of the bombykol cell in olfactory sensillum of *Bombyx mori*: voltage- and current-clamp analysis. J Insect Physiol 41: 451–455

Rospars J-P, Lánský P, Tuckwell HC, Vermeulen A (1996) Coding of odor in a steady-state deterministic model of an olfactory receptor neuron. J Comput Neurosci 3: 51–72

Schild D, Restrepo D (1998) Transduction mechanisms in vertebrate olfactory receptor cells. Physiol Rev 78: 429–466

Steinbrecht RA (1999) Olfactory receptors. In: Eguchi E, Tominaga Y (eds) Atlas of arthropod sensory receptors. Springer, Berlin Heidelberg New York Tokyo, pp 155–176

Thurm U, Küppers J (1980) Epithelial physiology in insect sensilla. In: Locke M, Smith DS (eds) Insect biology in the future. Academic Press, New York, pp 735–763

Tuckwell HC (1988) Introduction to theoretical neurobiology, vol 1. Cambridge University Press, Cambridge

Vermeulen A, Rospars J-P (1998a) Dendritic integration in olfactory sensory neurons: a steady-state analysis of how the neuron structure and neuron environment influence the coding of odor intensity. J Comput Neurosci 5: 243–266

Vermeulen A, Rospars J-P (1998b) A simple analytical method for determining the steady-state potential in models of geometrically complex neurons. J Neurosci Methods 82: 123–133

Zufall F, Hatt H (1991) Dual activation of sex pheromone-dependent ion channel from insect olfactory dendrites by protein kinase C activators and cyclic GMP. Proc Natl Acad Sci USA 88: 8520–8524